

# Green Rust and Iron Oxide Formation Influences Metolachlor Dechlorination during Zerovalent Iron Treatment

TUNLAWIT SATAPANAJARU

Department of Environmental Science, Kasetsart University, Bangkok, Thailand 10900

PATRICK J. SHEA\* AND  
STEVE D. COMFORT

School of Natural Resources, University of Nebraska, Lincoln, Nebraska 68583-0915

YUL ROH

Environmental Sciences Division, Oak Ridge National Laboratory, Oak Ridge, Tennessee 37831-6038

Electron transfer from zerovalent iron ( $\text{Fe}^0$ ) to targeted contaminants is affected by initial  $\text{Fe}^0$  composition, the oxides formed during corrosion, and surrounding electrolytes. We previously observed enhanced metolachlor destruction by  $\text{Fe}^0$  when iron or aluminum salts were present in the aqueous matrix and Eh/pH conditions favored formation of green rusts. To understand these enhanced destruction rates, we characterized changes in  $\text{Fe}^0$  composition during treatment of metolachlor with and without iron and aluminum salts. Raman microspectroscopy and X-ray diffraction (XRD) indicated that the iron source was initially coated with a thin layer of magnetite ( $\text{Fe}_3\text{O}_4$ ), maghemite ( $\gamma\text{-Fe}_2\text{O}_3$ ), and wüstite ( $\text{FeO}$ ). Time-resolved analysis indicated that akaganeite ( $\beta\text{-FeOOH}$ ) was the dominant oxide formed during  $\text{Fe}^0$  treatment of metolachlor. Goethite ( $\alpha\text{-FeOOH}$ ) and some lepidocrocite ( $\gamma\text{-FeOOH}$ ) formed when  $\text{Al}_2(\text{SO}_4)_3$  was present, while goethite and magnetite ( $\text{Fe}_3\text{O}_4$ ) were identified in  $\text{Fe}^0$  treatments containing  $\text{FeSO}_4$ . Although conditions favoring formation of sulfate green rust (GR(II);  $\text{Fe}_6(\text{OH})_{12}\text{SO}_4$ ) facilitated  $\text{Fe}^0$ -mediated dechlorination of metolachlor, only adsorption was observed when GR(II) was synthesized (without  $\text{Fe}^0$ ) in the presence of metolachlor and Eh/pH changed to favor  $\text{Fe}(\text{III})$ oxyhydroxide or magnetite formation. In contrast, dechlorination occurred when magnetite or natural goethite was amended with  $\text{Fe}(\text{II})$  (as  $\text{FeSO}_4$ ) at pH 8 and continued as long as additional  $\text{Fe}(\text{II})$  was provided. While metolachlor was not dechlorinated by GR(II) itself during a 48-h incubation, the GR(II) provided a source of  $\text{Fe}(\text{II})$  and produced magnetite (and other oxide surfaces) that coordinated  $\text{Fe}(\text{II})$ , which then facilitated dechlorination.

## Introduction

The popularity of zerovalent metals for treating groundwater contaminants has prompted a variety of studies to elucidate the mechanisms of contaminant destruction. While electron

release from the  $\text{Fe}^0$  core is undoubtedly the primary source of reducing power, the nature of the oxide layers formed on the iron surface will influence subsequent electron-transfer reactions. In  $\text{Fe}^0$ -batch experiments, exposure of bare  $\text{Fe}^0$  for direct electron transfer likely occurs only when the  $\text{Fe}^0$  grain is mechanically scratched through agitation. Most of the  $\text{Fe}^0$  surface will be covered with an oxide film, and its composition can have a dramatic influence on electron-transfer properties. Long-term batch, column and field studies with zerovalent iron have shown that the oxide layer will evolve with time into a complex mixture of amorphous iron oxides, iron oxide salts, and other mineral precipitates (1–4).

For reduction reactions to proceed, electrons must flow from the iron-solution interface to the organic contaminant (electron acceptor). While there is supporting evidence for a variety of electron-transfer mechanisms, including direct electron transfer (5), mediated electron transfer (6), or catalytic hydrogenation (7), a growing body of literature supports the role of surface-complexed  $\text{Fe}(\text{II})$  as a major reductant in the transformation of several types of contaminants (8–13). The predominant mechanism is contingent upon environmental conditions and the oxides formed. By understanding the characteristics of these oxides and the conditions (Eh/pH) under which they are favored, manipulation of the soil–water environment to enhance contaminant destruction may be possible.

Metolachlor (2-chloro-*N*-(2-ethyl-6-methylphenyl)-*N*-(2-methoxy-1-methylethyl)acetamide) is one of the most widely used chloroacetamide herbicides in agronomic crops. It was among four pesticides extensively monitored in the National Alachlor Well Water Survey which included more than 6 million private and domestic wells (14). Metolachlor was detected in about 1% of the wells sampled in that study and has been found in surface waters in 14 states (15). Although classified as slightly toxic (Toxicity Class III), metolachlor is a suspected teratogen, mutagen, and carcinogen (15). These observations substantiate a need to remediate chloroacetamide-contaminated water and soil.

Zerovalent iron has been shown to dechlorinate metolachlor and alachlor (2-chloro-*N*-(2,6-diethylphenyl)-*N*-(methoxymethyl)acetamide) (16–18). Following a metolachlor spill at a local agricultural cooperative, we conducted a field-scale remediation experiment and treated contaminated soil in large windrows with  $\text{Fe}^0$ . By adding  $\text{Al}_2(\text{SO}_4)_3$  (a common soil acidifying agent) with  $\text{Fe}^0$ , metolachlor destruction was significantly greater than with  $\text{Fe}^0$  alone (99% versus 72% within 90 d (17)). Beneath the surface of the treated windrows, metolachlor-contaminated soils that received  $\text{Fe}^0$  and  $\text{Al}_2(\text{SO}_4)_3$  displayed a green-blue color indicative of green rust. Soils exhibiting the green rust color (inside the windrow) had lower metolachlor concentrations than soils at the surface (more oxidized and brown in color). Subsequent laboratory batch experiments confirmed that adding Al,  $\text{Fe}(\text{II})$ , or  $\text{Fe}(\text{III})$  salts with  $\text{Fe}^0$  greatly increased metolachlor and nitrate destruction kinetics (19, 20). A common observation from these salt-amended  $\text{Fe}^0$  treatments was the initial formation of green rust (mixed  $\text{Fe}(\text{II})/\text{Fe}(\text{III})$  double hydroxide). Moreover, when Al was added, loss of Al from solution corresponded with release of  $\text{Fe}(\text{II})$ . Because several color changes (i.e., green, yellow, brown, black) indicative of different oxides were noted during these experiments (19) and it is known that the nature and composition of iron oxides affect electron transfer, we sought to identify the oxides formed during corrosion of  $\text{Fe}^0$  in the presence of Al and Fe salts under varying oxygen conditions and determine their influence on metolachlor dechlorination.

\* Corresponding author phone: (402)472-1533; fax: (402)472-7904; e-mail: pshea@unl.edu.

## Experimental Section

**Formation of Iron Oxides During Metolachlor Transformation.** To determine changes in iron oxide mineralogy associated with metolachlor reduction, we repeated batch solution experiments with Fe<sup>0</sup> amended with Al<sub>2</sub>(SO<sub>4</sub>)<sub>3</sub> and FeSO<sub>4</sub> which were previously shown to dechlorinate metolachlor (17–19). Annealed Fe<sup>0</sup> (formed by indirect heating under a reducing atmosphere) was used because metolachlor destruction rates were greater with salt-amended annealed Fe<sup>0</sup> than with unannealed iron (19). Peerless annealed iron (Peerless Metal Powders, Detroit, MI) with a surface area of 0.134 m<sup>2</sup> g<sup>-1</sup> (Micromeritics, Norcross, GA) was used in all experiments. The source of Al<sub>2</sub>(SO<sub>4</sub>)<sub>3</sub> was a commercial soil acidifier (Dragon Chemical Corp., Roanoke, VA) containing 17% Al and 48% SO<sub>4</sub>. The FeSO<sub>4</sub> (as 99.8% FeSO<sub>4</sub>·7H<sub>2</sub>O) was obtained from Fisher Scientific (Pittsburgh, PA). All chemicals and materials were used as received.

Metolachlor was prepared in deionized distilled water (conductivity = 17.4–19.0 MΩ; carbonates ≤0.4 mM) from the commercial product Dual 8E (Syngenta, Greensboro, NC). The initial metolachlor concentration varied between 1.06 and 1.41 mM as determined by comparison with a high purity standard (Syngenta). The metolachlor solution (100 mL) was treated with Fe<sup>0</sup>, Fe<sup>0</sup> + Al<sub>2</sub>(SO<sub>4</sub>)<sub>3</sub>, Fe<sup>0</sup> + FeSO<sub>4</sub>, or Fe<sup>0</sup> + Al<sub>2</sub>(SO<sub>4</sub>)<sub>3</sub> + FeSO<sub>4</sub>. Concentrations of the amendments included 50 g L<sup>-1</sup> (5% w/v) of Fe<sup>0</sup>, 5 g (0.5% w/v) of Dragon Al<sub>2</sub>(SO<sub>4</sub>)<sub>3</sub> (31.5 mM Al<sup>3+</sup> and 25.0 mM SO<sub>4</sub><sup>2-</sup>), and 10 g L<sup>-1</sup> (1.0% w/v) of Fisher FeSO<sub>4</sub> (35.9 mM Fe<sup>2+</sup> and SO<sub>4</sub><sup>2-</sup>). Flasks were covered with Parafilm and agitated up to 48 h on an orbital shaker at 25 °C. To mimic oxygen conditions encountered during our field-scale treatment of metolachlor-contaminated soil (17) and because green rust was not readily observed with these experimental treatments under anaerobic conditions (19), experimental units were agitated under aerobic conditions. At preselected times, multiple 1.2-mL aliquots were removed and transferred to 1.5-mL polypropylene microcentrifuge tubes, centrifuged at 13000 × *g* for 10 min, and analyzed by high performance liquid chromatography (HPLC). Tests indicated no significant adsorption of metolachlor on the glassware or microcentrifuge tubes. Samples of the Fe<sup>0</sup>-metolachlor suspensions were removed from the batch reactors at 2, 4, 8, and 12 h, filtered through 0.22-μm filter paper, and preserved under N<sub>2</sub> for X-ray diffraction (XRD) analysis.

Metolachlor analysis was performed with HPLC by injecting 20 μL of sample into a 4.6- by 250-mm Keystone Betasil NA column (ThermoHypersil-Keystone, Bellefonte, PA) connected to a Shimadzu (Kyoto, Japan) photodiode array detector with quantification at 220 nm. The mobile phase was 50:50 CH<sub>3</sub>CN–water at a flow rate of 1 mL min<sup>-1</sup>. Concentrations of metolachlor and dechlorinated metolachlor (2'-ethyl-6'-methyl-*N*-(methoxyprop-2-yl)acetamide) were determined by comparison with high purity standards (Syngenta). Under these conditions, typical retention times were 12 min for metolachlor and 8 min for dechlorinated metolachlor. Chloride analysis was conducted with a Dionex DX-120X ion chromatograph (Sunnyvale, CA) using an AS14 IonPac column and sodium carbonate-bicarbonate eluent.

XRD was used to monitor temporal changes in mineralogy and was performed with a Scintag XDS 2000 diffractometer (Scintag, Sunnyvale, CA) operating at a scan rate of 2E 2θ min<sup>-1</sup>. Cobalt K-α radiation (40 kV, 40 mA) was used to minimize fluorescence of Fe-rich minerals. The iron metal was also characterized by Raman microspectroscopy (PM Electrochem, Ontario, Canada). Raman spectra were obtained with a Renishaw 1000 microscope system with a CCD detector (400 × 600 pixels) using a 30 mW He Ne laser.

**Experiments with Green Rust.** Because rapid metolachlor destruction coincided with green rust formation (ref 19 and

herein), three separate experiments were conducted to evaluate the effects of green rust on this process. In the first procedure (Experiment I), green rust was synthesized within an Eh-pH stat, and metolachlor disappearance was monitored after changing Eh and pH to values outside the stability region of green rust. The second procedure synthesized and freeze-dried GR(II) and used known masses of GR(II) to determine destruction kinetics (Experiment II). The third procedure created conditions favoring green rust formation *in the presence of Fe<sup>0</sup>*, then removed the Fe<sup>0</sup>, and followed metolachlor loss in the green rust suspensions under aerobic and anaerobic conditions (Experiment III). Specific experimental details are provided below as Green Rust Experiments I, II, and III.

**Green Rust Experiment I.** Detailed descriptions of the Eh-pH stat components and configuration are provided elsewhere (21, 22). A Metrohm titrino pH-stat (Brinkman Instruments Inc., Westbury, NY) was used to measure, control, and regulate pH within the reaction cell. The pH stat continuously dispenses small volumes of acid (HCl) or base (NaOH) into the reaction cell to maintain the preset pH. Redox potential is controlled by a potentiostat (21), which maintains redox within ±0.02 V. This is accomplished by monitoring the analogue signal from a redox probe (Corning, Bigflats, NY) and based on the preselected Eh, relaying an electrical signal to one of two solenoid valves, which allows gas to pass into the reaction cell from cylinders containing compressed air or H<sub>2</sub>/Ar (3%/97%).

For this experiment, aqueous solutions containing 125.0 mM FeSO<sub>4</sub> and 1.41 mM metolachlor were placed in the reaction cell and held at pH 7 and an Eh of -0.3 V. The observed formation of green rust under these conditions is consistent with previous studies and lies within the region of metastability with Fe<sub>3</sub>O<sub>4</sub> (23). After green rust formed, the batch reactors were equilibrated for 1 h, and then ambient conditions were changed from an Eh of -0.3 V and pH 7 to (i) Eh = -0.3 V and pH 4, (ii) Eh = -0.6 V and pH 11, or (iii) Eh = +0.3 V and pH 7 in three separate experiments. Once Eh/pH was changed, solution samples were periodically removed for 24 h and changes in metolachlor concentrations determined.

**Green Rust Experiment II.** Batch experiments were then conducted to determine how green rust affects the reaction of metolachlor with Fe<sup>0</sup> and Fe(II). The GR(II) was synthesized in an anaerobic glovebox (Coy Laboratory Products, Grass Lake, MI) which maintained O<sub>2</sub> concentration below 100 ppm. GR(II) was prepared by continuously mixing a 5:1 solution of 125.0 mM FeSO<sub>4</sub> with 25.0 mM FeCl<sub>3</sub>, then titrating with 0.5 M NaOH to pH 7 with the pH-stat. Once pH 7 was achieved, the solution was allowed to equilibrate for 2–3 h and filtered through a 0.22 μm filter. The filtrate was freeze-dried for 24 h and characterized by XRD. Freeze-dried GR(II) was added to a 0.35 mM metolachlor solution in the anaerobic chamber and temporal changes in metolachlor concentration were determined. Treatments included the following: (i) 40 g L<sup>-1</sup> GR(II); (ii) 40 g L<sup>-1</sup> GR(II) + 4 g L<sup>-1</sup> FeSO<sub>4</sub>; (iii) 40 g L<sup>-1</sup> GR(II) + 10 g L<sup>-1</sup> Fe<sup>0</sup>; (iv) 10 g L<sup>-1</sup> Fe<sup>0</sup>; and (v) 10 g L<sup>-1</sup> Fe<sup>0</sup> + 40 g L<sup>-1</sup> FeSO<sub>4</sub>.

**Green Rust Experiment III.** A third experimental procedure determined the reactivity of green rust suspensions formed during Fe<sup>0</sup> corrosion following Fe<sup>0</sup> removal. XRD analysis confirmed GR(II) formation in a 1.41 mM metolachlor solution within 2 h after mixing 50 mg annealed Fe<sup>0</sup> with 10 mg L<sup>-1</sup> FeSO<sub>4</sub> under aerobic conditions. Similar conditions were created using 50 g L<sup>-1</sup> Fe<sup>0</sup> + 10 g L<sup>-1</sup> FeSO<sub>4</sub> (35.9 mM Fe<sup>2+</sup> and SO<sub>4</sub><sup>2-</sup>) and 50 g L<sup>-1</sup> Fe<sup>0</sup> + 10 g L<sup>-1</sup> FeSO<sub>4</sub> + 5 g L<sup>-1</sup> Al<sub>2</sub>(SO<sub>4</sub>)<sub>3</sub> (35.9 mM Fe<sup>2+</sup>, 31.5 mM Al<sup>3+</sup>, and 60.9 mM SO<sub>4</sub><sup>2-</sup>). After 2 h, a strong magnet was placed under the treatment flasks (*n* = 3) and the suspension decanted. Temporal changes in metolachlor concentrations and Cl<sup>-</sup> release were followed

in paired treatments where the Fe<sup>0</sup> was and was not removed. A second experiment followed identical procedures, but after 2 h of treatment the reactors were transferred to an anaerobic chamber, the Fe<sup>0</sup> was removed, and temporal changes in metolachlor concentrations were determined.

**Metolachlor Transformation by Fe(II) on Iron Oxides.** Because different iron oxides formed during Fe<sup>0</sup>-mediated metolachlor destruction, we sought to determine whether metolachlor could be transformed by Fe(II) associated with these oxides. Oxides included goethite, lepidocrocite ( $\gamma$ -FeOOH), hematite ( $\alpha$ -Fe<sub>2</sub>O<sub>3</sub>) (Bayer, Pittsburgh, PA), and magnetite (Fe<sub>3</sub>O<sub>4</sub>) (Fisher). BET surface areas were 13.7 m<sup>2</sup> g<sup>-1</sup> (goethite), 15.9 m<sup>2</sup> g<sup>-1</sup> (lepidocrocite), 5.6 m<sup>2</sup> g<sup>-1</sup> (magnetite), and 11.2 m<sup>2</sup> g<sup>-1</sup> (hematite) (Micromeritics, Norcross, GA). For comparison, a natural source of goethite (referred to as natural goethite) was also used in some experiments. This natural goethite had a BET surface area of 1.5 m<sup>2</sup> g<sup>-1</sup> (Micromeritics). Acid-extractable and total metal contents of the goethites were compared using EPA Method 3050b with inductively coupled argon plasma analysis (ICAP) (Midwest Laboratories, Inc., Omaha, NE) and energy-dispersive X-ray (EDX) analysis (University of Nebraska-Lincoln Soil and Plant Analytical Laboratory).

Amorphous (poorly crystalline) ferric oxide was prepared by neutralizing a 0.4 M solution of FeCl<sub>3</sub>·6H<sub>2</sub>O (Fisher) with 1 M NaOH and washing twice with distilled water. The poorly crystalline gel was freeze-dried. The amorphous iron oxide product had a characteristic broad XRD peak at 15° 2 $\theta$  and a BET surface area (Micromeritics) of 158.3 m<sup>2</sup> g<sup>-1</sup>.

Because of observed pH differences and the demonstrated importance of pH in surface- and Fe(II)-mediated reduction reactions (8, 13), we first determined the influence of pH on metolachlor transformation by oxide-associated Fe(II). This was accomplished by adding 5 g of natural goethite and 5 g of FeSO<sub>4</sub> (179.5 mM Fe<sup>2+</sup> and SO<sub>4</sub><sup>2-</sup>) to 100 mL of a 0.35 mM metolachlor solution inside the anaerobic chamber and holding the pH at 6, 7, and 8 with a pH-stat. Samples were periodically collected during a 24-h experiment, and metolachlor concentrations were determined by HPLC. Because pH 8 was most effective in transforming metolachlor, subsequent experiments were performed at pH 8. We compared goethite sources by conducting identical batch experiments (5 g of goethite + 5 g of FeSO<sub>4</sub> in 100 mL of solution) and measuring metolachlor transformation along with chloride release and characterizing the goethite surfaces with XRD. The reactivities of pure goethite (Bayer), lepidocrocite, amorphous ferric oxide, and magnetite were also compared by adding FeSO<sub>4</sub> under identical conditions.

To determine why metolachlor transformation ceased in the magnetite + FeSO<sub>4</sub> treatment after several hours, a separate experiment was conducted in which an additional 2 g of FeSO<sub>4</sub> (71.8 mM Fe<sup>2+</sup>) was added to 100 mL suspensions containing 5 g of magnetite in 0.33 mM metolachlor solution after 6, 12, and 24 h. Metolachlor concentrations and chloride release were determined as previously described.

Adsorption of metolachlor to the oxides was determined by adding 5 g of the minerals to 50-mL Teflon centrifuge tubes with 30 mL of deionized distilled water containing 0.04, 0.18, 0.35, 0.70, 1.06, and 1.41 mM metolachlor in a 3 mM CaCl<sub>2</sub> matrix. The tubes were equilibrated on a reciprocating shaker at 25 °C for 24 h. At 24 h, 1.2-mL aliquots were removed and analyzed as previously described. Adsorbed metolachlor was calculated from the difference between initial and equilibrium solution concentrations.

## Results and Discussion

**Metolachlor Destruction and Iron Oxide Formation.** We previously observed near stoichiometric dechlorination of metolachlor during treatment with Fe<sup>0</sup> + Al<sub>2</sub>(SO<sub>4</sub>)<sub>3</sub> based on measurement of Cl<sup>-</sup>, the appearance of dechlorinated

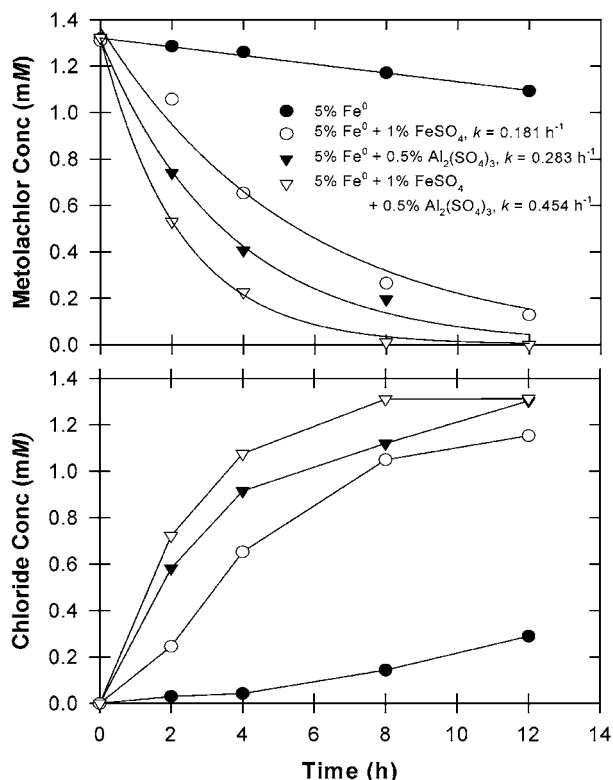


FIGURE 1. Changes in metolachlor concentration (A) and chloride release (B) following treatment with 50 g L<sup>-1</sup> Fe<sup>0</sup> (5% w/v) and Fe<sup>0</sup> + 5 g L<sup>-1</sup> Al<sub>2</sub>(SO<sub>4</sub>)<sub>3</sub> (0.5% w/v) or Fe<sup>0</sup> + 10 g L<sup>-1</sup> FeSO<sub>4</sub> (1% w/v).

metolachlor, and <sup>14</sup>C mass balance (17, 18). Subsequent work indicated faster kinetics when Al<sub>2</sub>(SO<sub>4</sub>)<sub>3</sub> was used with Fe<sup>0</sup> over AlCl<sub>3</sub>, Fe<sub>2</sub>(SO<sub>4</sub>)<sub>3</sub>, or FeCl<sub>3</sub>, although all of these salts were more effective than Fe<sup>0</sup> alone (19). That study and experiments conducted herein showed the fastest metolachlor destruction when Al<sub>2</sub>(SO<sub>4</sub>)<sub>3</sub> and FeSO<sub>4</sub> were both added with Fe<sup>0</sup> (Figure 1A). Chloride analysis indicated dechlorination in all treatments with negligible losses due to adsorption (Figure 1B). The appearance of green rust in several of the most effective treatments prompted an investigation into the oxides formed during Fe<sup>0</sup> oxidation and their impacts on metolachlor transformation.

Raman microspectroscopy and XRD analysis revealed that the Peerless annealed iron was initially coated with a thin layer of magnetite (Fe<sub>3</sub>O<sub>4</sub>), maghemite ( $\gamma$ -Fe<sub>2</sub>O<sub>3</sub>), and wüstite (FeO). Mineralogical analysis indicated formation of akaganeite ( $\beta$ -FeOOH), goethite ( $\alpha$ -FeOOH), lepidocrocite ( $\gamma$ -FeOOH), magnetite, and GR(II) in the presence of these salts (Table 1). When no salts were added to the Fe<sup>0</sup>-batch systems, akaganeite was the primary mineral observed. The poorly crystalline akaganeite has been observed in Fe<sup>0</sup> barriers and is considered stable under reducing conditions (4). GR(II) was prevalent for 8 h when FeSO<sub>4</sub> was added to the Fe<sup>0</sup> batch reactor. However, when Al<sub>2</sub>(SO<sub>4</sub>)<sub>3</sub> was used, goethite was identified within 2 h and lepidocrocite within 12 h. A greenish-blue color indicative of green rust was observed within the first 2 h, but green rust could not be confirmed by XRD. Roh et al. (24) and Pecher et al. (13) similarly reported difficulty in identifying green rust by XRD when only traces were present or the green rust exhibited a pseudohexagonal form. Misawa et al. (25) further proposed that the green solution complex may be converted to goethite and lepidocrocite without precipitation of GR(II), making detection of this intermediate phase difficult.

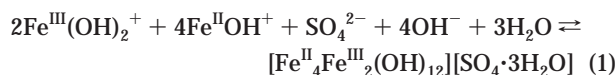
Green rusts are known to occur as intermediate phases in the formation of iron oxides during oxidation of Fe(II) in

TABLE 1. Mineral Identification by Time-Resolved XRD Analysis of Fe<sup>0</sup>-Metolachlor Suspensions

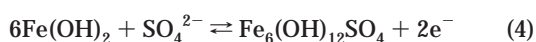
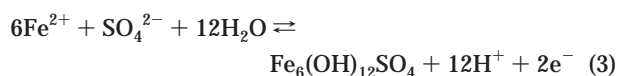
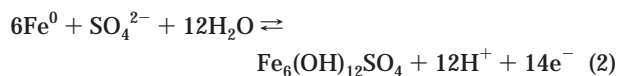
treatment		time (h)			
		2	4	8	12
annealed Fe <sup>0</sup>		ND <sup>a</sup>	akaganeite	akaganeite	akaganeite
	pH <sup>b</sup>	7.93 (8.46)	8.12 (7.91)	8.19 (7.43)	8.22 (7.33)
	Eh (V) <sup>c</sup>	-0.076	-0.124	-0.144	-0.162
annealed Fe <sup>0</sup> + Al <sub>2</sub> (SO <sub>4</sub> ) <sub>3</sub>		akaganeite	akaganeite	goethite	goethite
	pH	5.15 (4.75)	5.84 (6.29)	5.71 (6.06)	5.76 (6.05)
	Eh	+0.156	+0.080	+0.121	+0.118
annealed Fe <sup>0</sup> + FeSO <sub>4</sub>		green rust (II)	green rust (II)	green rust (II)	goethite
	pH	6.75 (7.03)	6.93 (7.00)	7.12 (6.99)	7.14 (7.07)
	Eh	-0.336	-0.320	-0.319	-0.354
annealed Fe <sup>0</sup> + Al <sub>2</sub> (SO <sub>4</sub> ) <sub>3</sub> + FeSO <sub>4</sub>		akaganeite	akaganeite	goethite	goethite
	pH	5.96 (4.95)	6.02 (6.27)	6.15 (6.16)	6.32 (6.09)
	Eh	+0.109	-0.051	-0.071	-0.068

<sup>a</sup> Not determined. <sup>b</sup> Solution pH at time of XRD analysis. <sup>c</sup> Approximate Eh at time of XRD analysis based on continuous monitoring of Eh (and corresponding parenthetic pH values) in a separate experiment.

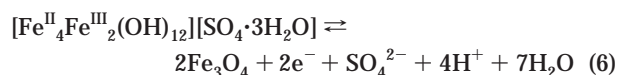
neutral and alkaline solutions (10, 23, 26). They can be found during corrosion of iron in permeable reactive barriers (3, 27), in groundwater rich in Fe(II) (28), and in anoxic soils (26). The composition of GR(II) is approximately [Fe<sup>II</sup><sub>4</sub>Fe<sup>III</sup><sub>2</sub>(OH)<sub>12</sub>]<sup>2+</sup>[SO<sub>4</sub>·nH<sub>2</sub>O]<sup>2-</sup> with an average Fe oxidation number of 2.33 (29, 30). GR(II) is believed to form by the reaction of Fe<sup>III</sup>(OH)<sub>2</sub><sup>+</sup> with Fe<sup>II</sup>OH<sup>+</sup> and SO<sub>4</sub><sup>2-</sup> and is composed of Fe(II) and Fe(III) held together by ol- and oxo-bridges formed during consumption of OH<sup>-</sup> ((25, 31, 32) eq 1):



Complexation of sulfate with Fe(III) slows down the formation of goethite, which occurs through polymerization of Fe(OH)<sub>2</sub><sup>+</sup> at pH 4–7 (33, 34). Green solution complexes may initially form (25). We previously reported the appearance of green-colored solutions during treatment of metolachlor with Fe<sup>0</sup> + FeSO<sub>4</sub> at near-neutral pH and at a lower pH when Al<sub>2</sub>(SO<sub>4</sub>)<sub>3</sub> was also present (19). Under reducing conditions GR(II) may be in equilibrium with Fe<sup>0</sup>, Fe<sup>2+</sup>, or Fe(OH)<sub>2</sub> (eqs 2–4 (26)):

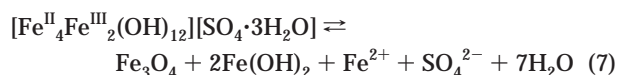


Magnetite (Fe<sup>II</sup>Fe<sup>III</sup><sub>2</sub>O<sub>4</sub>) was identified in the Fe<sup>0</sup> + FeSO<sub>4</sub> treatment after 8 h (Table 1). Magnetite may form from oxidation of Fe(OH)<sub>2</sub> (eq 5) or GR(II) (eq 6):



Unlike passivating Fe(III) oxides, magnetite allows charge transfer through the Fe<sup>0</sup>/Fe<sub>3</sub>O<sub>4</sub> interface, and reduction reactions can continue but at a lower rate than with the bare

metal (35). Green rust is metastable with respect to magnetite except within a limited domain near neutral pH when Fe<sup>2+</sup><sub>(aq)</sub> ≥ 0.1 M where it is the stable phase (23, 26). Tamaura et al. (31) demonstrated GR(II) dissolution and precipitation as magnetite under an N<sub>2</sub> atmosphere (i.e., conversion without oxidation). This reaction releases Fe<sup>2+</sup> when magnetite is produced (eq 7):



Magnetite formation in our Fe<sup>0</sup> + FeSO<sub>4</sub> treatments may be explained via green rust metastability with respect to magnetite because the Eh remained below -0.3 V and pH at sampling was between 6.75 and 7.14 for the 12-h experiment (Table 1).

Although a common oxidation product of GR(II) is lepidocrocite (eq 8)



goethite was more prevalent when Al<sub>2</sub>(SO<sub>4</sub>)<sub>3</sub> was added and appeared within 2 h (Table 1). The overall lower rate of Fe(II) oxidation in the presence of Al favors goethite as the end product rather than lepidocrocite (36–38). Moreover, the presence of Al may produce mixed Al–Fe phases (37). The mechanism likely involves precipitation of Al(OH)<sub>3</sub>, which causes precipitation and hydrolysis of Fe(II) at a lower pH than in the absence of Al(OH)<sub>3</sub>, producing an Al-substituted green rust which is isostructural with Al-free green rust but more resistant to oxidation (36, 39). Continued oxidation yields Al-substituted goethite (37). Taylor (38) further suggested that the presence of Al increases the solubility of Fe(III) hydroxy species at pH > 4.0, accompanied by an increase in Eh, which was observed in our treatments containing Al (Table 1). In Taylor's experiments, the Fe(III) precipitated as the hydroxy species at pH 4 reverted to a colloidal solution in the presence of Al, and the increased Fe(III) solubility was attributed to formation of a mixed Fe(III)-Al(III) hydroxy species. The presence of sulfate also tends to slow transformation of the poorly crystalline Fe(III) forms to the more highly structured goethite (34, 40).

**Green Rust Experiment I.** The appearance of green rust caused by aluminum or iron salt additions (Table 1) during Fe<sup>0</sup> treatment resulted in faster metolachlor dechlorination

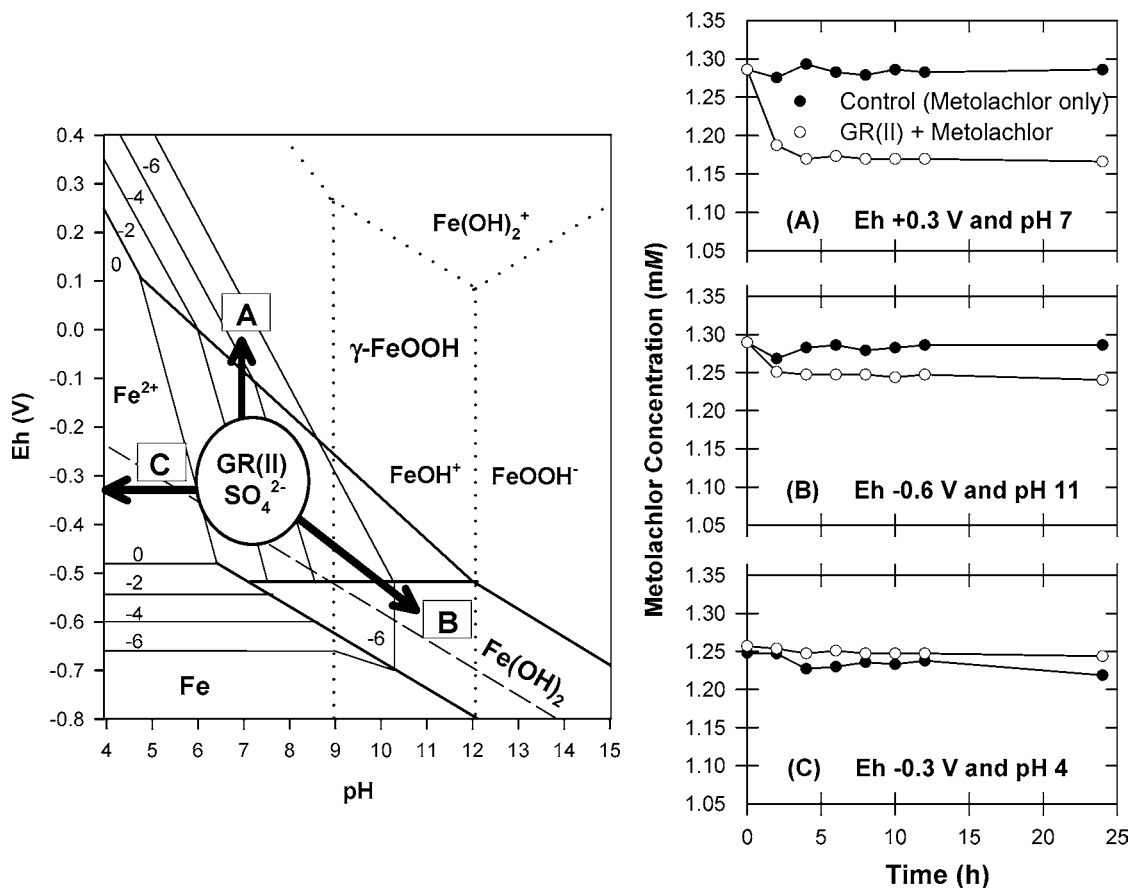


FIGURE 2. Eh-pH diagram showing the stability field of GR(II) under varying Fe(II) concentrations ( $10^{-7}$  M) and a  $\text{SO}_4^{2-}$  activity = 0.1 M (adapted from ref 26). Graphs A, B, and C show changes in metolachlor concentrations following shifts in Eh/pH.

rates over  $\text{Fe}^0$  alone (19). We determined the ability of green rust to reduce metolachlor by synthesizing GR(II) (in the absence of  $\text{Fe}^0$ ) and monitoring metolachlor after adjusting Eh and pH outside the stability region of green rust. Control treatments indicated that metolachlor was stable under the various Eh/pH conditions imposed. When the Eh was increased to 0.3 V (pH 7), the suspension turned yellow-brown (generally indicative of goethite or lepidocrocite formation expected under aerobic conditions), and the metolachlor concentration decreased (Figure 2A). A high chloride background due to  $\text{FeCl}_3$  used in the green rust synthesis precluded quantification of chloride release, but no dechlorinated metolachlor was detected (via HPLC). Based on previous results where dechlorination of metolachlor ( $\text{Cl}^-$  release) only occurred when the dechlorinated product was observed (18), we believe the loss of metolachlor is primarily adsorption to the Fe(III) oxyhydroxides formed when the Eh of the system was increased and oxidation of GR(II) occurred.

Inducing conditions favoring  $\text{Fe}(\text{OH})_2$  precipitation (Eh = -0.6 V and pH = 11) appeared to stabilize the green rust and even less change in metolachlor concentration was observed (Figure 2B). Simply lowering the pH of the green rust suspension to 4.0 dissolved the green rust but did not produce other oxides at Eh = -0.3 and had no effect on metolachlor (Figure 2C).

**Green Rust Experiment II.** XRD analysis confirmed that GR(II) was produced from the synthesis procedure employed (Figure 3A). By working with freeze-dried GR(II), a known mass of GR(II) was used to treat metolachlor, but results indicated only a small decrease in metolachlor concentration within 48 h (Figure 3B). This decrease is believed due to adsorption, but dechlorination cannot be ruled out based on the small concentration change. However, when the GR(II) was mixed with  $\text{Fe}^0$  ( $10 \text{ mg L}^{-1}$ ), destruction kinetics were

greatly enhanced above that observed with  $\text{Fe}^0$  alone (Figure 3B). Similar results were observed when  $\text{FeSO}_4$  was used with  $\text{Fe}^0$  in place of GR(II). No metolachlor transformation occurred in the absence of  $\text{Fe}^0$  with GR(II) +  $\text{FeSO}_4$  in an unbuffered solution (pH 4.5–4.9; Figure 3B) or at pH 8.0 (data not shown). Adsorption of Fe(II) on the green rust would likely induce dissolution (41) and may explain why no metolachlor transformation was observed. Our observations indicate that the synthesized GR(II) itself was not directly responsible for metolachlor transformation during this 48-h experiment but was providing a source of Fe(II) for iron oxide-mediated transformation of metolachlor.

**Green Rust Experiment III.** Because colloidal precipitates indicative of green rust suspensions were observed in the  $\text{Fe}^0 + \text{FeSO}_4 + \text{Al}_2(\text{SO}_4)_3$  treatment and this treatment produced the fastest reaction kinetics under ambient aerobic conditions, we again created conditions favoring green rust formation in the presence of  $\text{Fe}^0$ , then removed the  $\text{Fe}^0$ , and compared temporal changes in metolachlor concentration and  $\text{Cl}^-$  release in the suspension for 48 h under aerobic and anaerobic conditions. By adding  $\text{Fe}^0$  to aqueous metolachlor, dissolved oxygen was quickly removed; however, when the iron was removed from the reactor, oxygen diffused back into the suspension and raised the Eh. This resulted in the suspension only maintaining the green rust color for <1 h. Nevertheless, for the  $\text{Fe}^0 + \text{FeSO}_4$  treatment, the metolachlor concentration continued to decline for 8 h after the iron was removed before reaching a plateau (Figure 4). Some  $\text{Cl}^-$  release was detected during this decline (Figure 4), but the total amount released quickly reached a plateau after the  $\text{Fe}^0$  was removed and on a molar basis only corresponded to approximately 25% of the metolachlor lost. Dechlorination in the aerobic system is likely associated with Fe(II)-oxide interactions, but dechlorination could not be sustained due

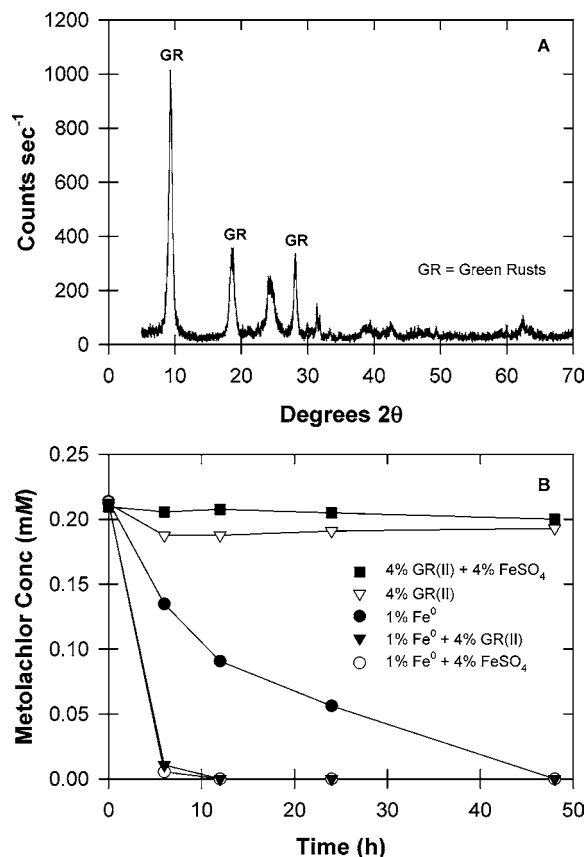


FIGURE 3. (A) XRD analysis of synthesized GR(II). (B) Changes in metolachlor concentration following treatment with freeze-dried GR(II) (with and without 10 g L<sup>-1</sup> Fe<sup>0</sup> (1% w/v) or 40 g L<sup>-1</sup> (4% w/v) FeSO<sub>4</sub>).

to depletion of Fe(II) once the Fe<sup>0</sup> was removed. Thus metolachlor loss under these conditions was primarily due to adsorption on the iron oxides and is similar to what we observed by raising the Eh of GR(II) suspensions (Green Rust Experiment I, Figure 2A).

In comparison to the Fe<sup>0</sup> + FeSO<sub>4</sub> treatment, the addition of Al<sub>2</sub>(SO<sub>4</sub>)<sub>3</sub> resulted in approximately 70% of the metolachlor being transformed before the Fe<sup>0</sup> was removed (Figure 4). After removing the Fe<sup>0</sup>, the metolachlor concentration decreased at a much lower rate than in the Fe<sup>0</sup> + FeSO<sub>4</sub> treatment, but chloride measurements indicated more of the metolachlor lost from solution was dechlorinated in the treatment containing aluminum. These results are consistent with our observations of enhanced metolachlor transformation by Fe<sup>0</sup> in the presence of Al salts (ref 19 and Figure 1 herein).

In treatments where the batch reactors were open to the atmosphere for 2 h then transferred to the anaerobic chamber before removing the Fe<sup>0</sup> (Figure 4C), solutions maintained a green color for nearly 24 h. While subsequent metolachlor loss in the Fe<sup>0</sup> + FeSO<sub>4</sub> treatment (after Fe<sup>0</sup> removal) was less under anaerobic than under aerobic conditions, metolachlor loss on a molar basis was more stoichiometric with Cl<sup>-</sup> release (i.e., less loss due to adsorption; Figure 4, A vs B and C vs D). It should be noted that when the entire experiment was performed inside the anaerobic chamber, metolachlor transformation was much slower, and no green coloration was observed in the suspensions (data not shown). In that instance no further decrease in metolachlor concentration was observed after the Fe<sup>0</sup> was removed. These results again indicate that GR(II) facilitates metolachlor dechlorination when Fe<sup>0</sup> is present, but, by itself, GR(II) is not a strong reductant of metolachlor.

Although green rusts have been shown to promote reduction of contaminants such as Cr(VI) (42, 43), nitrate (44, 45), nitrite (29), and selenate (46), differences in reaction kinetics among chlorinated aliphatic compounds have been observed and linked to degree of chlorination. Erbs et al. (10) observed similar first-order rate constants for transformation of CCl<sub>4</sub> by Fe<sup>0</sup> and GR(II), but the reaction of GR(II) with CHCl<sub>3</sub> was 100 times slower. This is consistent with increasing rates of reduction as halogenation increases (47). Thus a very slow rate of reaction with green rust is anticipated for a monochlorinated compound such as metolachlor, resulting in insignificant dechlorination within the short time frame of our experiments.

#### Metolachlor Transformation by Fe(II) on Iron Oxides.

Researchers have demonstrated transformation of nitroaromatics and chlorocarbons on mineral oxides in the presence of structural or surficial Fe(II) (8, 11, 13, 48–50), and strong correlations have been observed between Fe<sup>2+</sup>(aq) concentration and nitrate reduction by Fe<sup>0</sup> (20). Recognizing that GR(II) is transitory and that various oxides form during treatment of metolachlor with Fe<sup>0</sup> depending on Eh/pH and surrounding electrolytes (Table 1), we investigated metolachlor transformations by Fe(II) on magnetite, lepidocrocite, hematite, amorphous ferric hydroxide, and two sources of goethite. Supportive (S-type) isotherms indicated low metolachlor adsorption with little difference among the oxides at initial concentrations below 1.06 mM (data not shown). At 1.41 mM, the metolachlor adsorption coefficients (K<sub>d</sub>) were 0.56 L kg<sup>-1</sup> for goethite and 0.31 L kg<sup>-1</sup> for magnetite. The low affinity of metolachlor for the oxides would minimize adsorption to nonreactive sites which could decrease the overall rate of reductive transformation, as demonstrated for nitroaromatic compounds (50).

When we combined goethite with FeSO<sub>4</sub> under varying pH (6–8), the metolachlor concentration decreased at pH 8.0 (Figure 5A) while little change was observed at pH 6 or 7 (not shown). Based on Cl<sup>-</sup> release, metolachlor loss is primarily attributed to dechlorination (Figure 5B). No dechlorination was observed in the absence of FeSO<sub>4</sub>. Lee and Batchelor (48) similarly reported an increase in the rate of trichloroethylene dechlorination by GR(II) as pH was increased from 6.8 to 8.1. This was attributed to conversion of nonreactive sites to reactive Fe(II) sites and the higher electron density of deprotonated (≡Fe<sup>III</sup>OFe<sup>II</sup>OH<sup>0</sup>) than protonated (≡Fe<sup>III</sup>OFe<sup>II</sup>OH<sub>2</sub><sup>+</sup>) surface groups (51). Following an initial drop in metolachlor concentration, we observed a lag before metolachlor decreases occurred again when natural goethite was used. The biphasic loss indicates a change in the reactivity and/or composition of the oxide surface. Pecher et al. (13) attributed the increased rate of polyhalogenated methane reduction with exposure time to rearrangement of initially sorbed Fe(II) species to more reactive forms.

Little change in metolachlor concentration was observed when lepidocrocite or hematite (not shown) was used with FeSO<sub>4</sub> (Figure 6A). This contrasts with a rapid decrease in metolachlor concentration when treated with magnetite + FeSO<sub>4</sub> and amorphous ferric oxide + FeSO<sub>4</sub>, reaching a plateau within 12 h or less. Chloride release was detected in these treatments, but the amounts were too small to obtain reliable data. When we repeated the experiment and added more FeSO<sub>4</sub> (71.8 mM Fe<sup>2+</sup>) to the magnetite-metolachlor suspensions at 6, 12, and 24 h, metolachlor concentrations continued to decline, with near-stoichiometric release of chloride (Figure 6B). These observations indicate that the lack of available Fe(II) was the reason metolachlor concentrations failed to continue to decrease after the initial treatment (Figure 6A).

Side by side comparisons showed that the natural goethite + FeSO<sub>4</sub> was more effective than pure goethite in dechlorinating metolachlor (Figure 5A,B). XRD analysis indicated

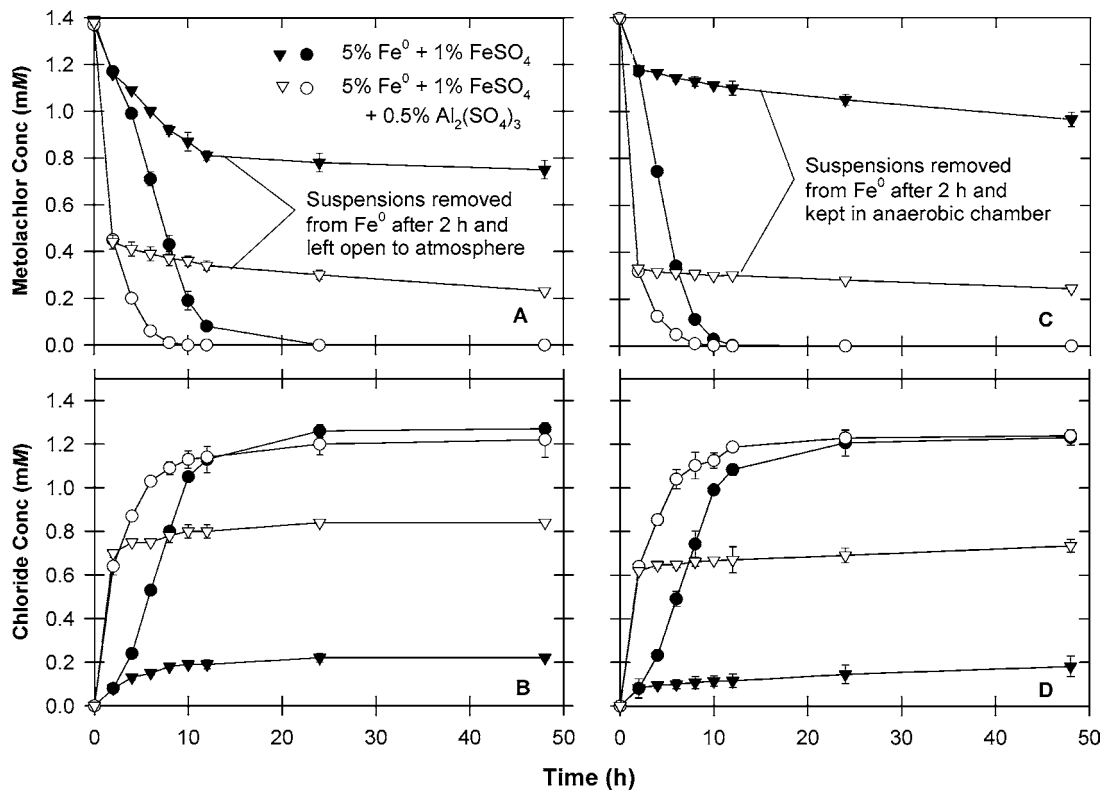


FIGURE 4. Changes in metolachlor and  $\text{Cl}^-$  concentrations following treatment with  $50 \text{ g L}^{-1} \text{Fe}^0$  (5% w/v) or  $\text{Fe}^0 + 10 \text{ g L}^{-1} \text{FeSO}_4$  (1% w/v) or  $\text{Fe}^0 + \text{FeSO}_4 + 5 \text{ g L}^{-1} \text{Al}_2(\text{SO}_4)_3$  (0.5% w/v) under anaerobic and aerobic conditions. Paired treatments show the effects of removing  $\text{Fe}^0$  from the batch reactors and maintaining suspensions under aerobic or anaerobic conditions.

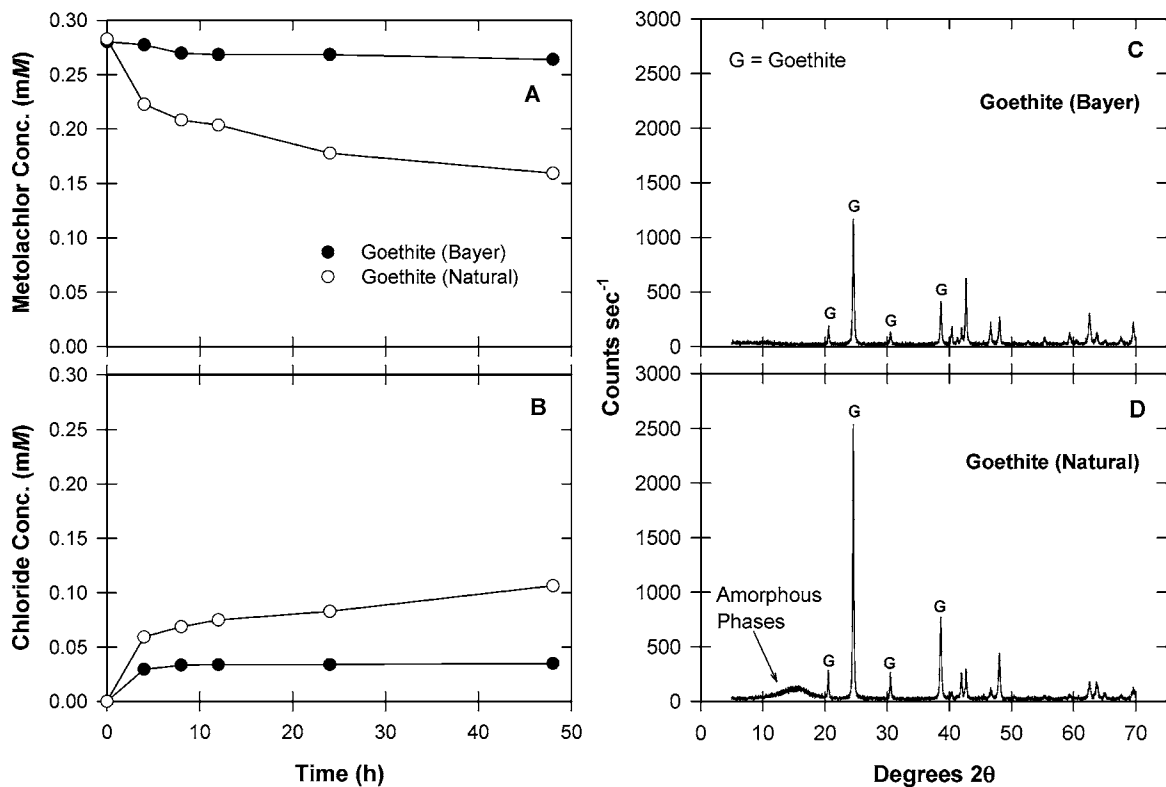


FIGURE 5. Comparison of goethite sources (natural vs Bayer) on metolachlor concentrations (A) and  $\text{Cl}^-$  release (B) following treatment with  $50 \text{ g L}^{-1}$  goethite +  $50 \text{ g L}^{-1} \text{FeSO}_4$  at pH 8.0. (C and D) XRD analyses of the goethite sources.

that the natural goethite also contains amorphous ferric oxide (Figure 5 (part D vs C)). The greater reactivity of the natural

goethite may be due in part to the presence of the amorphous oxide, which reacted with  $\text{Fe}^{2+}$  to form magnetite (Figure 7).

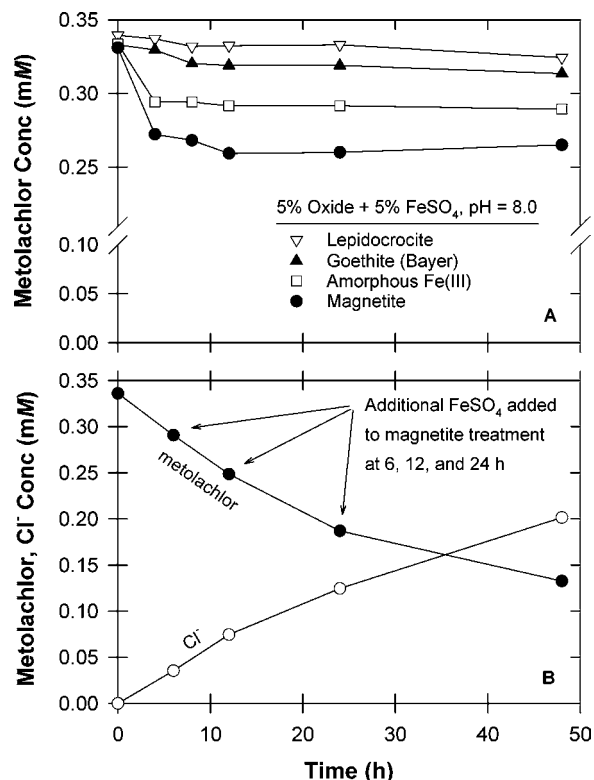
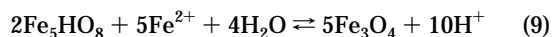


FIGURE 6. (A) Changes in metolachlor concentration following treatment with 50 g L<sup>-1</sup> Bayer goethite, lepidocrocite, amorphous Fe(III) oxide, and magnetite + 50 g L<sup>-1</sup> FeSO<sub>4</sub> at pH 8.0. (B) Effects of multiple FeSO<sub>4</sub> additions (20 g L<sup>-1</sup> FeSO<sub>4</sub> added at 6, 12, and 24 h) on metolachlor loss and chloride release following treatment with magnetite + FeSO<sub>4</sub> at pH 8.0.

Magnetite has similarly been shown to form from the reaction of poorly crystalline ferrihydrite with Fe<sup>2+</sup> (eq 9 (53–55)):



EDX analysis further revealed that the natural goethite contained approximately 0.22% aluminum, while none was detected in the pure (Bayer) goethite. The natural goethite also contained greater acid-extractable iron and aluminum concentrations than Bayer goethite (82 181 vs 42 mg kg<sup>-1</sup> Fe and 687 vs 32 mg kg<sup>-1</sup> Al), both of which can promote Fe(II) precipitation and hydrolysis to produce reactive Fe(II) sites on the oxide surface (52, 56). As with pure magnetite, it is likely that consumption of Fe<sup>2+</sup> similarly limited the reactivity of magnetite produced from amorphous oxide present in the natural goethite.

Mann et al. (54) reported a green rust intermediate in the conversion of ferrihydrite to magnetite. This observation likely reflects equilibria between green rust and amorphous ferric oxides, in which a lowering of pH releases Fe(OH)<sub>2</sub><sup>+</sup> ions from green rust which can then form amorphous precipitates at pH > 7 (31). However, poorly crystalline iron oxides may also be transformed to hematite (which was not reactive under our experimental conditions) or goethite, the latter of which is favored by aging solutions containing FeSO<sub>4</sub> (57). Thus competing reactions yielding oxides that are less surface-reactive than magnetite may have limited the effectiveness of amorphous ferric oxide + FeSO<sub>4</sub> in our experiments.

Other researchers have observed differences in reactivity among oxides. Schultz and Grundl (58) compared the reduction rates of 4-chloronitrobenzene by Fe(II) on goethite, montmorillonite, silica, and alumina. They attributed differences in reactivity to the inherent capacities of the mineral

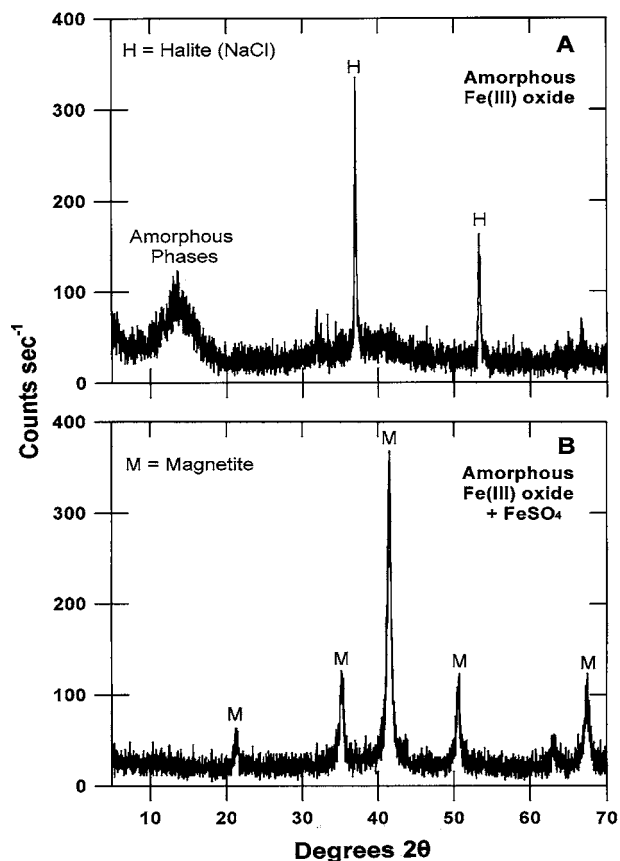


FIGURE 7. XRD analysis of amorphous Fe(III) oxide before (A) and after (B) treatment with FeSO<sub>4</sub>.

surfaces to dehydrate Fe(II) and form inner-sphere complexes. Moreover, the nature of the complex was suggested to influence reactivity, with Fe(II)-ferric oxide (i.e., goethite) being much more reactive than Fe(II)-silica oxide or Fe(II)-alumina (58). Pecher et al. (13) reported the density of surface hydroxyl groups (total number per nm<sup>2</sup>) of lepidocrocite (1.67) < goethite (5.5) < magnetite (9.4). This order of hydroxyl group density does not correspond with surface areas but follows the order of reactivity observed among the oxides used in our experiments. Amonette et al. (11) suggested that Fe(II) in close proximity on the surface may promote the multiple electron transfers typical of dechlorination reactions. The differences in reactivity among the iron oxides in our experiments are also consistent with Vikesland and Valentine (59), who calculated overall rate coefficients of 501 ± 436 and 340 ± 31 L M<sup>-1</sup> m<sup>-2</sup> min<sup>-1</sup> for reduction of monochloramine (NH<sub>2</sub>Cl) by Fe(II) on magnetite and goethite. Comparative rate coefficients were an order of magnitude smaller for lepidocrocite, hematite, and ferrihydrite.

Our results indicate that the capacity of Fe<sup>0</sup> as a reductant for metolachlor is maximized under conditions that maintain a nonpassivating, reactive surface on the iron. The formation of magnetite, which conducts electrons, is preferred over goethite, which passivates the Fe<sup>0</sup> surface. Green rusts are metastable with respect to magnetite, which was identified in Fe<sup>0</sup> treatments containing FeSO<sub>4</sub>. The appearance of green rust during Fe<sup>0</sup> oxidation coincided with conditions favorable for metolachlor reduction. While metolachlor was not reduced by GR(II) alone or supplemented with FeSO<sub>4</sub> within the time frame of our experiments, this observation does not preclude dechlorination under conditions where green rusts may persist for extended time periods, such as in hydro-morphic soils (26, 60). Previous research has demonstrated

the potential of green rusts to control Fe<sup>2+</sup> activity in solution (23, 26), and our experiments indicated that GR(II) provides a source of Fe(II) which can form reactive complexes on oxide surfaces. Conversion of GR(II) to magnetite produced an oxide surface conducive to metolachlor transformation, and metolachlor was dechlorinated by reactions with Fe(II) coordinated on magnetite and natural goethite. The reaction of poorly crystalline Fe(III) oxides present in natural goethite with Fe(II) produced magnetite and metolachlor was dechlorinated. Aside from dechlorination through reaction with Fe<sup>0</sup>, our results indicate the potential of surface-bound Fe(II) to reduce chloroacetamides. Metolachlor dechlorination may be promoted by creating conditions resulting in formation of oxides with a high density of reactive surface sites and under which sufficient Fe<sup>2+</sup> is available. The appearance of green rust was a good indicator of these conditions.

## Acknowledgments

We thank Dr. Marek Odziemkowski (University of Waterloo, Ontario, Canada) for Raman microspectroscopic analysis, Dr. Michelle Scherer (University of Iowa) for assistance in GR(II) synthesis, and Thomas A. Machacek (University of Nebraska) for technical assistance. This research was supported by EPA/EPSCoR proj. R-829422-010, the Nebraska Research Initiative, and University of Nebraska Water Center. Paper no. 13971 is a contribution of Agric. Res. Div. proj. NEB-40-002 and 019.

## Literature Cited

- (1) Gillham, R. W.; O'Hannesin, S. F. *Ground Water* **1994**, *32*, 958–967.
- (2) Agrawal, A.; Tratnyek, P. G. *Environ. Sci. Technol.* **1996**, *30*, 153–160.
- (3) Scherer, M. M.; Balko, B. A.; Tratnyek, P. G. In *Mineral-Water Interfacial Reactions: Kinetics and Mechanisms*; Sparks, D. L., Grundl, T. J., Eds; ACS Symp. Ser. 715, American Chemical Society: Washington, DC, 1998; pp 301–322.
- (4) Phillips, D. H.; Gu, B.; Watson, D. B.; Roh, Y.; Liang, L.; Lee, S. Y. *Environ. Sci. Technol.* **2000**, *34*, 4169–4176.
- (5) Scherer, M. M.; Westall, J. C.; Ziomek-Moroz, M.; Tratnyek, P. G. *Environ. Sci. Technol.* **1997**, *31*, 2385–2391.
- (6) Weber, E. J. *Environ. Sci. Technol.* **1996**, *30*, 716–719.
- (7) Odziemkowski, M. S.; Gui, L.; Gillham, R. W. *Environ. Sci. Technol.* **2000**, *34*, 3495–3500.
- (8) Klausen, J.; Tröber, S. P.; Haderlein, S. B.; Schwarzenbach, R. P. *Environ. Sci. Technol.* **1995**, *29*, 2396–2404.
- (9) Haderlein, S. B.; Pecher, K. In *Mineral-Water Interfacial Reactions: Kinetics and Mechanisms*; Sparks, D. L., Grundl, T. J., Eds; ACS Symp. Ser. 715, American Chemical Society: Washington, DC, 1998; Chapter 17.
- (10) Erbs, M.; Hansen, H. C. B.; Olsen, C. E. *Environ. Sci. Technol.* **1999**, *33*, 307–311.
- (11) Amonette, J. E.; Workman, D. J.; Kennedy, D. W. *Environ. Sci. Technol.* **2000**, *34*, 4606–4613.
- (12) Hwang, I.; Batchelor, B. *Environ. Sci. Technol.* **2000**, *34*, 5017–5022.
- (13) Pecher, K.; Haderlein, S. B.; Schwarzenbach, R. P. *Environ. Sci. Technol.* **2002**, *36*, 1734–1741.
- (14) Holden, L.; Graham, J. A. *Environ. Sci. Technol.* **1992**, *26*, 935–943.
- (15) U. S. Environmental Protection Agency. *Pesticide Fact Sheet Number 106: Metolachlor*; Office of Pesticides and Toxic Substances: Washington, DC, 1987; pp 10–101.
- (16) Eykholt, G. R.; Davenport, D. T. *Environ. Sci. Technol.* **1998**, *32*, 481–487.
- (17) Comfort, S. D.; Shea, P. J.; Machacek, T. A.; Gaber, H.; Oh, B.-T. *J. Environ. Qual.* **2001**, *30*, 1636–1643.
- (18) Gaber, H. M.; Comfort, S. D.; Shea, P. J.; Machacek, T. A. *J. Environ. Qual.* **2002**, *31*, 962–969.
- (19) Satapanajaru, T.; Comfort, S. D.; Shea, P. J. *J. Environ. Qual.* **2003**, *32*, 1726–1734.
- (20) Huang, Y.; Zhang, T. C.; Shea, P. J.; Comfort, S. D. *J. Environ. Qual.* **2003**, *32*, 1306–1315.
- (21) Petrie, R. A.; Grossl, P. R.; Sims, R. C. *Soil Sci. Soc. Am. J.* **1998**, *62*, 379–382.
- (22) Singh, J.; Comfort, S. D.; Shea, P. J. *Environ. Sci. Technol.* **1999**, *33*, 1488–1494.

- (23) Refait, Ph.; Génin, A.; Abdelmoula, M.; Génin, J.-M. R. *Corrosion Sci.* **2003**, *45*, 659–676.
- (24) Roh, Y.; Lee, S. Y.; Elless, M. P. *Environ. Geol.* **2000**, *40*, 184–194.
- (25) Misawa, T.; Hashimoto, K.; Shimodaira, S. *Corrosion Sci.* **1974**, *14*, 131–149.
- (26) Génin, J.-M. R.; Bourrié, G.; Trolard, F.; Abdelmoula, M.; Jaffrezic, A.; Refait, P.; Maitre, V.; Humbert, B.; Herbillon, A. *Environ. Sci. Technol.* **1998**, *32*, 1058–1068.
- (27) Gu, B.; Phelps, T. J.; Liang, L.; Dickey, M. J.; Roh, Y.; Kinsall, B. L.; Palumbo, A. V.; Jacobs, G. K. *Environ. Sci. Technol.* **1999**, *33*, 2170–2177.
- (28) Koch, C. B.; Morup, S. *Clay Miner.* **1991**, *26*, 577–582.
- (29) Hansen, H. C.; Borggaard, O. K.; Sørensen, J. *Geochim. Cosmochim. Acta* **1994**, *58*, 2599–2608.
- (30) Génin, J.-M. R.; Olowe, A. A.; Refait, Ph.; Simon, L. *Corrosion Sci.* **1996**, *38*, 1751–1762.
- (31) Tamaura, Y.; Yoshida, T.; Katsura, T. *Bull. Chem. Soc. Jpn.* **1984**, *7*, 2411–2416.
- (32) Murray, J. W. In *Marine Minerals. Reviews in Mineralogy*; Burns, R. G., Ed.; Mineralogical Society of America: Washington, DC, pp 47–48.
- (33) Stucki, J. W.; Goodman, B. A.; Schwertmann, U. *Iron in Soils and Clay Minerals*; D. Riedel Pub. Co.: Boston, MA, 1988.
- (34) Baltpurvins, K. A.; Burns, R. C.; Lawrence, G. A. *Environ. Sci. Technol.* **1996**, *30*, 939–944.
- (35) Odziemkowski, M. S.; Schuhmacher, T. T.; Gillham, R. W.; Reardon, E. J. *Corrosion Sci.* **1998**, *40*, 371–389.
- (36) Taylor, R. M.; Schwertmann, U. *Clays Clay Miner.* **1978**, *26*, 373–383.
- (37) Fey, M. V.; Dixon, J. B. *Clays Clay Miner.* **1981**, *29*, 91–100.
- (38) Taylor, R. M. In *Soil Colloids and Their Associations in Aggregates*; De Boodt, M., Hayes, M., Herbillon, A., Eds.; Plenum Press: New York, 1990; pp 85–103.
- (39) Taylor, R. M.; McKenzie, R. M. *Clays Clay Miner.* **1980**, *30*, 179–187.
- (40) Brady, K. S.; Bigham, J. M.; Jaynes, W. F.; Logan, T. J. *Clays Clay Miner.* **1986**, *34*, 266–274.
- (41) Ona-Nguema, G.; Abdelmoula, M.; Jorand, F.; Benali, O.; Génin, A.; Block, J.-C.; Génin, J.-M. R. *Environ. Sci. Technol.* **2002**, *36*, 16–20.
- (42) Loyaux-Lawniczak, S.; Refait, P.; Ehrhardt, J.-J. *Environ. Sci. Technol.* **2000**, *34*, 438–443.
- (43) Williams, A.; Scherer, M. M. *Environ. Sci. Technol.* **2001**, *35*, 3488–3494.
- (44) Hansen, H. C. B.; Koch, H.; Nancke-Krogh, H.; Borggaard, O. K.; Sørensen, J. *Environ. Sci. Technol.* **1996**, *30*, 2053–2056.
- (45) Hansen, H. C. B.; Koch, H. *Clay Miner.* **1998**, *33*, 87–101.
- (46) Myneni, S. C. B.; Tokunaga, T. K.; Brown, G. E. *Science* **1997**, *278*, 1106–1109.
- (47) Vogel, T. M.; Criddle, C. S.; McCarty, P. L. *Environ. Sci. Technol.* **1987**, *21*, 722.
- (48) Lee, W.; Batchelor, B. *Environ. Sci. Technol.* **2002**, *36*, 5348–5354.
- (49) Lee, W.; Batchelor, B. *Environ. Sci. Technol.* **2002**, *36*, 5147–5154.
- (50) Hofstetter, T.; Schwarzenbach, R. P.; Haderlein, S. B. *Environ. Sci. Technol.* **2003**, *37*, 519–528.
- (51) Butler, E. C.; Hayes, K. F. *Environ. Sci. Technol.* **1998**, *32*, 1276–1284.
- (52) Tamaura, H.; Goto, K.; Nagayama, M. *Corrosion Sci.* **1976**, *16*, 197–207.
- (53) Tamaura, Y.; Buduan, P. V.; Katsura, T. *J. Chem. Soc., Dalton Trans.* **1981**, 1807–1811.
- (54) Mann, S.; Sparks, N. H. C.; Couling, S. B.; Larcombe, M. C. *J. Chem. Soc., Faraday Trans. 1* **1989**, *85*, 3033–3044.
- (55) Tronc, E.; Belleville, P.; Jolivet, J.-P.; Livage, J. *Langmuir* **1992**, *8*, 313–319.
- (56) Bertsch, P. M.; Miller, W. P.; Anderson, A. A.; Zelazny, L. W. *Clays Clay Miner.* **1989**, *37*, 12–18.
- (57) Schwertmann, U.; Fischer, W. R. *Geoderma* **1973**, *10*, 237–247.
- (58) Schultz, C. A.; Grundl, T. J. *Environ. Sci. Technol.* **2000**, *34*, 3641–3648.
- (59) Vikesland, P. J.; Valentine, R. L. *Environ. Sci. Technol.* **2002**, *36*, 512–519.
- (60) Trolard, F.; Génin, J.-M.; Abdelmoula, M.; Bourrié, G.; Humbert, B.; Herbillon, A. *Geochim. Cosmochim. Acta* **1997**, *61*, 1107–1111.

Received for review February 4, 2003. Revised manuscript received September 9, 2003. Accepted September 11, 2003.

ES0303485